

Lack of riluzole efficacy in the progression of the neurodegenerative phenotype in a new conditional mouse model of striatal degeneration

Grzegorz Kreiner ^{Corresp., 1}, Katarzyna Rafa-Zabłocka ¹, Piotr Chmielarz ¹, Monika Bagińska ¹, Irena Nalepa ¹

¹ Institute of Pharmacology, Polish Academy of Sciences, Dept. Brain Biochemistry, Kraków, Poland

Corresponding Author: Grzegorz Kreiner
Email address: kreiner@if-pan.krakow.pl

Background. Huntington's disease (HD) is a rare familial autosomal dominant neurodegenerative disorder characterized by progressive degeneration of medium spiny neurons (MSNs) located in the striatum. Currently available treatments of HD are only limited to alleviating symptoms; therefore, high expectations for an effective therapy are associated with potential replacement of lost neurons through stimulation of postnatal neurogenesis. One of the drugs of potential interest for the treatment of HD is riluzole, which may act as a positive modulator of adult neurogenesis, promoting replacement of damaged MSNs. The aim of this study was to evaluate the effects of chronic riluzole treatment on a novel HD-like transgenic mouse model, based on the genetic ablation of the transcription factor TIF-IA. This model is characterized by selective and progressive degeneration of MSNs.

Methods. Selective ablation of TIF-IA in MSNs (TIF-IA^{D1RCre} mice) was achieved by Cre-based recombination driven by the dopamine 1 receptor (D1R) promoter in the C57Bl/6N mouse strain. Riluzole was administered for 14 consecutive days (5 mg/kg, i.p.; 1x daily) starting at 6 weeks of age. Behavioral analysis included a motor coordination test performed on 13-week-old animals on an accelerated rotarod (4 to 40 r.p.m.; 5 min). To visualize the potential effects of riluzole treatment, the striata of the animals were stained by immunohistochemistry (IHC) and/or immunofluorescence (IF) with Ki67 (marker of proliferating cells), neuronal markers (NeuN and MAP2), and specific markers associated with neurodegeneration (GFAP, 8OHdG). Additionally, the morphology of dendritic spines of neurons was assessed by a commercially available FD Rapid Golgi Stain™ Kit.

Results. A comparative analysis of IHC staining patterns with chosen markers for the neurodegeneration process in MSNs did not show an effect of riluzole on delaying the progression of MSN cell death despite an observed enhancement of cell proliferation as visualized by the Ki67 marker. A lack of a riluzole effect was also reflected by the behavioral phenotype associated with MSN degeneration. Moreover, the analysis of dendritic spine morphology did not show differences between mutant and control animals.

Discussion. Despite the observed increase in newborn cells in the subventricular zone (SVZ) after riluzole administration, our study did not show any differences between riluzole-treated and non-treated mutants, revealing a similar extent of the neurodegenerative phenotype evaluated in 13-week-old TIF-IA^{D1RCre} animals. This could be due to either the treatment paradigm (relatively low dose of riluzole used for this study) or the possibility that the effects were simply too weak to have any functional meaning. Nevertheless, this study is in line with others that question the effectiveness of riluzole in animal models and raise concerns about the utility of this drug due to its rather modest clinical efficacy.

1 **Author Cover Page**

2

3

4 **Lack of riluzole efficacy in the progression of the neurodegenerative phenotype in a new**
5 **conditional mouse model of striatal degeneration**

6

7 Grzegorz Kreiner^{1#}, Katarzyna Rafa-Zabłocka¹, Piotr Chmielarz¹, Monika Bagińska¹, Irena
8 Nalepa¹

9 ¹Institute of Pharmacology, Polish Academy of Sciences, Dept. Brain Biochemistry,

10 31-343 Kraków, Smętna street 12, Poland

11

12 #Corresponding Author:

13 Grzegorz Kreiner

14 e-mail: kreiner@if-pan.krakow.pl

15

16

17

18 **Abstract**

19

20 **Background.** Huntington's disease (HD) is a rare familial autosomal dominant
21 neurodegenerative disorder characterized by progressive degeneration of medium spiny neurons
22 (MSNs) located in the striatum. Currently available treatments of HD are only limited to
23 alleviating symptoms; therefore, high expectations for an effective therapy are associated with
24 potential replacement of lost neurons through stimulation of postnatal neurogenesis. One of the
25 drugs of potential interest for the treatment of HD is riluzole, which may act as a positive
26 modulator of adult neurogenesis, promoting replacement of damaged MSNs. The aim of this
27 study was to evaluate the effects of chronic riluzole treatment on a novel HD-like transgenic
28 mouse model, based on the genetic ablation of the transcription factor TIF-IA. This model is
29 characterized by selective and progressive degeneration of MSNs.

30 **Methods.** Selective ablation of TIF-IA in MSNs (TIF-IA^{D1RCre} mice) was achieved by Cre-based
31 recombination driven by the dopamine 1 receptor (D1R) promoter in the C57Bl/6N mouse strain.
32 Riluzole was administered for 14 consecutive days (5 mg/kg, i.p.; 1x daily) starting at 6 weeks of
33 age. Behavioral analysis included a motor coordination test performed on 13-week-old animals
34 on an accelerated rotarod (4 to 40 r.p.m.; 5 min). To visualize the potential effects of riluzole
35 treatment, the striata of the animals were stained by immunohistochemistry (IHC) and/or
36 immunofluorescence (IF) with Ki67 (marker of proliferating cells), neuronal markers (NeuN and
37 microtubule-associated protein-2, MAP2), and specific markers associated with
38 neurodegeneration (GFAP, 8OHdG). Additionally, the morphology of dendritic spines of
39 neurons was assessed by a commercially available FD Rapid Golgi Stain™ Kit.

40 **Results.** A comparative analysis of IHC staining patterns with chosen markers for the
41 neurodegeneration process in MSNs did not show an effect of riluzole on delaying the
42 progression of MSN cell death despite an observed enhancement of cell proliferation as
43 visualized by the Ki67 marker. A lack of a riluzole effect was also reflected by the behavioral
44 phenotype associated with MSN degeneration. Moreover, the analysis of dendritic spine
45 morphology did not show differences between mutant and control animals.

46 **Discussion.** Despite the observed increase in newborn cells in the subventricular zone (SVZ)
47 after riluzole administration, our study did not show any differences between riluzole-treated and

48 non-treated mutants, revealing a similar extent of the neurodegenerative phenotype evaluated in
49 13-week-old TIF-IA^{D1RCre} animals. This could be due to either the treatment paradigm (relatively
50 low dose of riluzole used for this study) or the possibility that the effects were simply too weak
51 to have any functional meaning. Nevertheless, this study is in line with others that question the
52 effectiveness of riluzole in animal models and raise concerns about the utility of this drug due to
53 its rather modest clinical efficacy.

54

55

56 Introduction

57 Huntington's disease (HD) is a rare (1:10000) familial autosomal dominant
58 neurodegenerative disorder caused by an expanded stretch of polyglutamine (polyQ) repeats in
59 the protein huntingtin (Hannan 2005) and characterized by progressive degeneration of medium
60 spiny neurons (MSNs) located in the striatum. The disease inevitably culminates with death and
61 cures to at least retard its progression are unavailable so far. Currently available treatments are
62 limited to alleviating some of the symptoms, mainly involuntary movements, associated with the
63 disease. Despite the known origin, there is a lack of understanding of the complex pathogenesis
64 of HD, which affects multiple functions and regulatory pathways, making the development of
65 efficient therapeutics challenging (Kazantsev & Hersch 2007). Classic pharmacological models
66 of HD are based on applying a neurotoxin, 3-nitropropionic acid (3-NP) (Tunez et al. 2010),
67 however this approach leads to immediate neuronal death, which substantially narrows the
68 opportunity to observe the pathological changes associated with the slow neurodegenerative
69 process. On the other hand, many transgenic animal models of HD, even though created by
70 replicating the same genetic malfunction directly responsible for HD in humans, do not fully
71 recapitulate the HD-like phenotype, including profound neuronal loss (or at least not to the
72 expected extent) (Kreiner 2015).

73 Designed cell therapies for neurodegenerative diseases are mostly based on the
74 replacement of lost neurons through transplantation or activation of neuronal progenitor cells
75 (Emsley et al. 2005). In rodent models of HD, induced neurogenesis in MSNs is thought to be
76 evoked primarily due to neuronal precursors derived from the subventricular zone (SVZ) of the
77 lateral ventricles. The SVZ represents the largest reservoir of adult stem-like progenitors and in
78 normal conditions gives rise to new olfactory bulb interneurons (Bonfanti & Peretto 2007).
79 Stimulation of postnatal neurogenesis is being considered as a potential therapeutic target in
80 several neurodegenerative diseases including HD (Abdipranoto et al. 2008; Lindvall & Kokaia
81 2010; Ransome et al. 2012). One of the drugs of potential interest for the treatment of HD is
82 riluzole, already approved for the treatment of amyotrophic lateral sclerosis (ALS) (Miller et al.
83 2012). Riluzole, by interfering with glutamatergic neurotransmission, reduces excitotoxicity and
84 acts as a positive modulator of adult neurogenesis, promoting replacement of damaged MSNs,
85 however, whether it has any clinical meaning remains not clear (Katoh-Semba et al. 2002;
86 Squitieri et al. 2008; Veyrac et al. 2009). It was also shown that riluzole treatment can result in

87 enhancement of damaged neurite formation potentially leading to functional recovery of
88 motoneurons in rat model of L4-6 root avulsion (Bergerot et al. 2004). Based on experimental
89 data coming from cell and animal research, the classic pharmacological mechanism of its action
90 is related to so-called excitotoxic hypothesis of neurodegeneration. Namely, riluzole can inhibit
91 the release of glutamic acid most likely due to the inactivation of voltage-dependent sodium
92 channels on glutamatergic nerve terminals, as well as activation of a G-protein-dependent
93 signaling pathways (Doble 1996). Another postulated mechanism associated with beneficial role
94 of riluzole application is related to observed increase of serum concentrations of brain-derived
95 neurotrophic factor (BDNF) (Katoh-Semba et al. 2002), which neurotrophic factor is known to
96 be significantly diminished in the brains of HD patients, and its level seems to be correlated with
97 diseases onset progression and severity (Gauthier et al. 2004). Moreover, riluzole was shown to
98 be effective in attenuating several clinically relevant symptoms in a variation of an animal MPTP
99 model representing the early phase of Parkinson's disease (PD) (Verhave et al. 2012).
100 Nevertheless, there are still concerns about its utility due to rather modest clinical efficacy
101 (Miller et al. 2012).

102 To address this question, we applied a novel approach using a mouse model of HD-like
103 phenotype, based on the activation of an endogenous suicide mechanism achieved by genetic
104 ablation of the transcription factor TIF-IA, an essential regulator of polymerase I activity
105 (Kreiner et al. 2013). Inactivation of TIF-IA blocks the synthesis of ribosomal RNA, leading to
106 nucleolar disruption and p53-mediated apoptosis (Yuan et al. 2005). Loss of TIF-IA in neuronal
107 progenitor cells results in mice born without a brain (Parlato et al. 2008), but when it is lost in
108 mature neurons, the major features of the neurodegenerative process are recapitulated. Namely,
109 inactivation of the TIF-IA gene in striatal MSNs (TIF-IA^{D1RCre} mice) recapitulates the
110 phenotypic alterations associated with selective striatal neurodegeneration (occurring in 13-
111 week-old mice), including increased oxidative damage and inflammatory response, finally
112 leading to MSN cell death and resulting in an HD-like phenotype (i.e., impairment of motion
113 control and clasping behavior) (Kreiner et al. 2013). In contrast to the majority of other models
114 of neurodegeneration, TIF-IA^{D1RCre}-mutant mice are characterized by the progressive
115 degeneration of targeted neurons over a long period of time (several weeks), mimicking the
116 typical hallmark of the disease (Kreiner et al. 2013).

117

118 **Materials & Methods**

119 The summary of experimental design is illustrated on the chart (**Fig. 1**).

120 ***Mice***

121 Selective ablation of TIF-IA in the MSNs (TIF-IA^{D1RCre} mice) was achieved by *Cre/loxP*
122 recombination in the C57Bl/6N mouse strain. Transgenic mice hosting Cre recombinase under
123 the dopamine 1 receptor (D1R) promoter were crossed with animals harboring the floxed TIF-IA
124 gene as described previously (Kreiner et al. 2013). Mutant TIF-IA^{D1RCre} mice were kept together
125 with their control (Cre-negative) littermates in self-ventilated cages (Allentown, USA) under
126 standard laboratory conditions (12 h light/dark cycle, food and water ad libitum). This study was
127 carried out in strict accordance with the recommendations in the Guide for the Care and Use of
128 Laboratory Animals of the National Institutes of Health. The protocol for the behavioral study
129 was approved by the Animal Ethical Committee at the Institute of Pharmacology, Polish
130 Academy of Sciences (Permit Number: 951, issued: June 28, 2012).

131 ***Drug treatment***

132 After genotyping, the 6-week-old mice were divided into 4 experimental groups: control+VEH
133 (con/VEH), control+RIL (con/RIL), mutant+VEH (mut/VEH), mutant+RIL (mut/RIL), receiving
134 either riluzole (RIL; 5 mg/kg, i.p.; Sigma-Aldrich Chemical Co., St. Louis, USA) or vehicle
135 (VEH; 10% DMSO) for 14 consecutive days (1x daily). These doses did not influence daily cage
136 normal behavior observed in riluzole and vehicle treated mice.

137 ***Behavioral analysis***

138 A coordination test was performed on 13-week-old animals on an accelerated rotarod (Ugo
139 Basile, Italy). The assessment was preceded by training session, 1 day before the experiment (5
140 minutes on the rotating rod, constant speed). During the experiment the time spent on the
141 accelerating rod (4 to 40 r.p.m. within 5 min) was measured. Additionally, the weight of the
142 animals was consistently monitored during the time of drug application and on the day before the
143 behavioral test.

144 ***Immunohistochemistry***

145 To visualize the potential effects of drug treatment, the striata of animals were subject to *post-*
146 *mortem* staining using immunohistochemistry (IHC) and/or immunofluorescence (IF) with
147 specific markers as described previously (Chmielarz et al. 2013; Kreiner et al. 2013). Briefly, the
148 mice were sacrificed by cervical dislocation, and their brains were excised, fixed overnight in 4%

149 paraformaldehyde (PFA), dehydrated, embedded in paraffin and sectioned on a rotary microtome
150 on 7 μm thick slices. Chosen sections from corresponding regions of the striatum in mutant and
151 control animals were incubated overnight at 4 °C with primary anti-NeuN (1:500, Millipore; cat.
152 no MAB377), anti-MAP2 (1:1000, Abcam; cat. no ab5392) anti-GFAP (1:500, Millipore, cat. no
153 AB5541), and anti-8OHdG (1:200, Millipore; cat. no AB5830) antibodies. Visualization of
154 antigen-bound primary antibodies was carried out using a proper biotinylated secondary antibody
155 together with the Avidin–Biotin Complex (ABC; Vector Laboratories, USA) followed by
156 diaminobenzidine treatment (DAB; Sigma-Aldrich, USA) or an anti-rabbit Alexa-488 or Alexa-
157 594-coupled secondary antibody (Invitrogen, USA). Quantification of Ki67 expression was done
158 by counting all Ki67-positive cells on adjacent sections from $n=4-6$ animals of each
159 genotype/treatment in a single-blind experiment (an investigator did not know which samples
160 belong to which genotype/treatment).

161 *Dendritic spine morphology*

162 Morphological analysis of dendritic spines was assessed as described previously (Chmielarz et
163 al. 2015). Briefly, following extraction, the brains were rinsed in distilled water, impregnated
164 with the use of the FD Rapid Golgi Stain™ Kit (FD NeuroTechnologies, USA), and incubated in
165 30% sucrose for 3-7 days. Vibratome (Leica, Germany) sections were cut to 100 μm thick and
166 mounted on Super Frost Plus slides (Thermo Scientific, USA) and stained using solutions
167 provided in the kit. The dendritic spines were counted on the dorsal striatum between Bregma
168 1.1 and 0.0. Dendritic spines were counted on at least 10 μm long fragments of 3rd and 4th row
169 dendrites. There were 3 pieces counted from each neuron and 5 neurons counted for each animal.
170 Only completely stained neurons not obscured by neighboring neurons within the striatum were
171 considered. Spine counting and optical imaging were performed by an experimenter blind to the
172 genotype of the animal on a Nikon Eclipse 50i (Nikon, Japan) equipped with a CCD camera
173 connected to a computer equipped with NIS Elements BR 30 software.

174 *Statistical analysis*

175 Statistical analysis was performed with Graph Pad Prism 5.01. Data were evaluated by 2-way
176 analysis of variance (2-way ANOVA) followed by Bonferroni test for comparison of biologically
177 relevant groups.

178 **Results**

179 **Enhancement of cell proliferation observed in TIF-IA^{D1Cre} mutant mice and after riluzole**
180 **treatment.**

181 The expression of Ki67 showed substantial enhancement in the region of the SVZ in non-
182 treated 9-week-old TIF-IA^{D1Cre} mice and all riluzole-treated animals (**Fig. 2A-B**). Double
183 immunofluorescent staining revealed that the number of cells labelled with Ki67 (marker of cell
184 proliferation) in SVZ co-localize with the MAP2 (microtubule-associated protein-2, neuronal
185 marker) positive cells. These cells co-localize with DAPI (marker for nuclear staining) as well
186 (**Fig. 2C**).

187 **Lack of riluzole efficacy on progression of MSNs cell death despite enhancement of cell**
188 **proliferation.**

189 A comparative analysis of immunohistochemical staining patterns with chosen markers
190 characteristic for neurodegenerative process in MSNs (marker for labeling mature neurons,
191 NeuN; an oxidative stress indicator marker, 8-hydroxydeoxyguanosine, 8OHdG; astrocyte
192 marker, GFAP) did not show any visual differences between 13-week-old mutant TIF-IA^{D1Cre}
193 mice with or without riluzole treatment (**Fig. 3A-C**). The expression of all of the above-
194 mentioned markers seems to be similar in the riluzole treated and non-treated TIF-IA^{D1Cre}-
195 mutant mice, showing comparable enhancement of inflammatory processes, oxidative stress and
196 neuronal loss.

197 **Lack of riluzole efficacy on the behavioral phenotype associated with MSN degeneration.**

198 Chronic riluzole administration did not prevent impaired motor coordination of 13-week-old
199 mutant TIF-IA^{D1Cre} mice as demonstrated by the rotarod test (**Fig. 4**). The riluzole
200 administration had no effect on control animals, while the different effect of the introduced
201 mutation is reflected in a 2-way ANOVA, which reveals a treatment (riluzole) x genotype
202 interaction for genotype [$F(131.38) = 80.39$ ($p < 0.0001$)] but not for riluzole itself.

203 **Riluzole does not affect dendritic spine morphology in TIF-IA^{D1Cre} mice.**

204 Our previous research done on TIF-IA^{D1Cre} mice clearly showed that although the
205 neurodegeneration (cell loss) is not observed earlier than in 13-week-old animals, some
206 symptoms of cellular impairment can be seen 2-4 weeks in advance (Kreiner et al. 2013). Taking
207 this into account, we checked whether chronic riluzole treatment could have any positive effects

208 on neural cell morphology. Nevertheless, the performed analysis of the morphology of dendritic
209 spines on 9-week-old animals (where no cell loss is observed yet) did not show any differences
210 between mutants and controls (**Fig. 5**). There was also no effect of riluzole application on
211 dendritic spine morphology in control animals.

212

213

214 **Discussion**

215 The objective of this research was supported by preliminary studies, in which we
216 observed an increase in cell proliferation within the SVZ in 9-week-old TIF-IA^{D1RCre} mice
217 suggesting the existence of neurogenesis (**Fig. 2A-B**). This finding is consistent with other
218 studies reporting increased neurogenesis in other models of progressive neurodegeneration
219 (Luzzati et al. 2011; Nato et al. 2015). This prompted us that the progressive TIF-IA-driven
220 neurodegeneration in these mice offers the unique advantage to study if, in such conditions, the
221 endogenous progenitors potentially involved in putative neuroprotective mechanisms can be
222 modulated by experimental treatments. However, when performed double staining with Ki67 and
223 NeuN within the SVZ in 9-week-old TIF-IA^{D1RCre} mice, we were not able to find any evidence of
224 co-localization. On the other hand, further immunofluorescent analysis revealed that the number
225 of cells labelled with Ki67 co-localize with the MAP2 neuronal marker (**Fig. 2C**). This may be
226 explained by the fact that MAP2 belongs to early markers of neuronal maturation, while NeuN is
227 a marker of mature neurons being expressed later on (Sarnat 2013).

228 To elucidate whether the putative further enhancement of adult neurogenesis induced by
229 chronic riluzole administration can have any positive influence on the progression of the
230 neurodegenerative phenotype observed in TIF-IA^{D1RCre} mice, we evaluated chosen markers of
231 neurodegeneration known to be differentially expressed in these mice at 13 weeks old, where the
232 cell loss starts to be clearly visible as described previously (Kreiner et al. 2013). Additionally, we
233 also screened their behavioral phenotype by assessing motor coordination. Despite an observed
234 increase in newborn cells in the SVZ after riluzole administration as visualized by Ki-67 staining
235 (an effective marker of proliferating cells (Kee et al. 2002)) (**Fig. 2**), neither experimental
236 approach showed any differences between riluzole-treated and non-treated mutants, revealing a
237 similar extent of the neurodegenerative phenotype evaluated in 13-week-old animals (**Fig. 3-4**).

238 The mice were characterized by the same expression of induced-GFAP and 8OHdG and
239 profoundly reduced staining intensity for NeuN in the striatum (**Fig. 3A-C**). This was reflected
240 by the impairment in motor coordination on the rotarod test, and again, no differences were
241 observed between riluzole- and vehicle-treated mutants (**Fig. 4**). Overall, these experiments did
242 not show any beneficial effects of riluzole administration on the progress of the mutation.

243 It seemed that further enhancement of this process by riluzole administration can bring
244 considerable benefits in the form of slowing down the progression of the mutation. Our
245 transgenic models based on the conditional ablation of transcription factor TIF-IA have already
246 been positively verified as a possible tool to study the mechanisms of action of other
247 pharmacotherapies. In particular, we showed that the progression of neurodegenerative
248 phenotype in the TIF-IA^{DATCre} mice (PD model) can be postponed by L-DOPA (Rieker et al.
249 2011) or reboxetine treatment (Rafa-Zabłocka et al. 2014).

250 It can be argued that either the treatment paradigm was not appropriate to achieve the
251 expected drug efficacy or the effects were simply too weak to have any functional meaning.
252 Regarding the first issue, the dose of riluzole in chronic experiments performed on rodents does
253 indeed range from 1 to 40 mg/kg (Besheer et al. 2009; Carbone et al. 2012; Fumagalli et al.
254 2006; Sepulveda et al. 1999), and is predominantly 20 mg/kg when used to evoke a neurogenesis
255 response. Therefore, the dose used in our experiment was in the lower range of the therapeutic
256 window. The reason for choosing this particular dose was determined by the lethargy and spastic
257 gait followed by a high mortality rate of the mice treated with 20 and 10 mg/kg. This problem
258 has also been reported by other researchers when rats were treated with similar doses and
259 exhibited locomotor ataxia and lethargy (Kitzman 2009; Simard et al. 2012). We presume that
260 this phenomenon is associated with the specific mouse strain (C57Bl/6N) rather than with the
261 introduced mutation since the problem affected both control and TIF-IA^{D1RCre} mice.
262 Nevertheless, it has to be emphasized that even the dose of 5 mg/kg was able to induce cell
263 proliferation within the SVZ region as visualized by Ki67 staining (**Fig. 2A**) and quantified
264 afterwards (**Fig. 2B**). Moreover, there are existing reports that prove a similar dose to be
265 effective (Kitzman 2009).

266 In addition, in order to evaluate whether riluzole can exert any influence on affected
267 MSNs, we performed a quantitative analysis of dendritic spine morphology at the stage when the
268 neurons were still present in the striata of TIF-IA^{D1RCre} mice. We analyzed 9-week-old mice, as

269 this is the stage where no cell loss has been observed but the cascade of molecular events leading
270 to degeneration has already been prompted (Kreiner et al. 2013). Nevertheless, this analysis did
271 not show any changes in dendritic spine morphology (**Fig. 5**), supporting the observation that
272 riluzole seems to not be effective in the investigated model.

273 Surprisingly, we were not able to find any abnormalities in the morphology of dendritic
274 spines in the non-treated TIF-IA^{D^{IR}Cre}-mutant mice despite the clear neurodegenerative
275 phenotype that has already been documented. This issue has not been addressed in our previous
276 work. However, the occurrence of such changes is not always correlated with neurodegeneration
277 (Dickstein et al. 2010) or may be a subsequent event. On the other hand, lack of spine pathology
278 might also be attributed to the relatively early stage of pathology observed in 9-week-old TIF-
279 IA^{D^{IR}Cre} mutants, as other authors have shown that spine pathology was present in late (36-weeks
280 old) (Spires et al. 2004), but not early (20-weeks old) (Nithianantharajah et al. 2009),
281 symptomatic stages of the R6/1 Huntington disease model.

282 The lack of analysis of other time points (i.e., 16-week-old animals or older) can be
283 regarded as a drawback of the experimental design. This is mainly due to the relatively low
284 number of animals in the cohort, which is restricted by current strict animal welfare regulations.
285 Nevertheless, since the phenotype of riluzole-treated TIF-IA^{D^{IR}Cre} mice is non-distinguishable
286 from untreated mutants (regarding both the behavioral and histological levels) at the age of 13
287 weeks (where the cells are already starting to degenerate), it would be hard to imagine that any
288 differences would be observed at a later period. Lack of differences at this pivotal stage does not
289 provide any strong support for the investigation of earlier time points, which could have been
290 interesting if we had observed findings differentiating the animals at 13 weeks. However
291 unlikely, it cannot be excluded that analysis of additional time points in-between 9-th and 13-th
292 week would differentiate the riluzole treated and non-treated animals.

293 In spite of expectations based on previously gathered evidence in preclinical studies and
294 the use of riluzole in clinics for the treatment of ALS, a recent study also yielded disappointing
295 results concerning this drug. Despite being an expensive drug, it does not stop the progression of
296 ALS and is not always well tolerated, making the efficacy of riluzole in the treatment of ALS
297 inconclusive (Ginsberg & Lowe 2002). Moreover, experiments performed on animal models
298 assessing riluzole as a potential treatment for HD and spinocerebellar ataxia (SCA) had no
299 beneficial effects (Hockly et al. 2006; Schmidt et al. 2016). In clinical trials of anti-HD

300 treatment, there was also no clear neuroprotective effect of riluzole administration, and its effects
301 were narrowed only to reduced chorea (Frank 2014). Thus, our study seems to be in line with
302 others that question the effectiveness of riluzole in animal models and raise concerns about the
303 utility of this drug due to its rather modest clinical efficacy (Limpert et al. 2013).

304

305 **Conclusions**

306 Despite an observed increase in newborn cells in the SVZ after riluzole administration,
307 our study did not show any differences between riluzole-treated and non-treated mutants,
308 revealing a similar extent of the neurodegenerative phenotype evaluated in 13-week-old TIF-
309 IA^{DIRCre} animals, a new transgenic model resembling HD-like neurodegeneration. This lack of an
310 observed effect could be due to either the treatment paradigm or the possibility that the effects
311 were simply too weak to have any functional meaning. Nevertheless, this study is in line with
312 others that question the effectiveness of riluzole in animal models and raise concerns about the
313 utility of this drug due to its rather modest clinical efficacy.

314

315 **Acknowledgements**

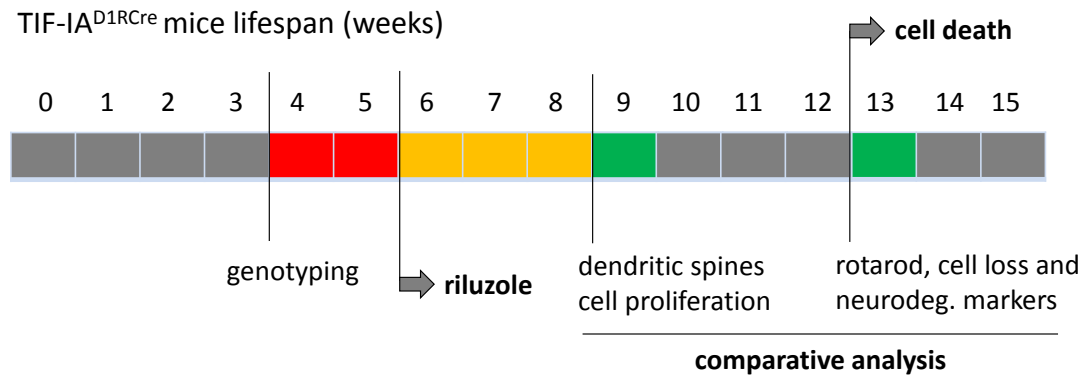
316 We thank Prof. Günther Schütz and Dr. Rosanna Parlato from the German Cancer Research
317 Center (DKFZ, Heidelberg, Germany) for their generous gift of the TIF-IA^{DIRCre} mice.

318

319

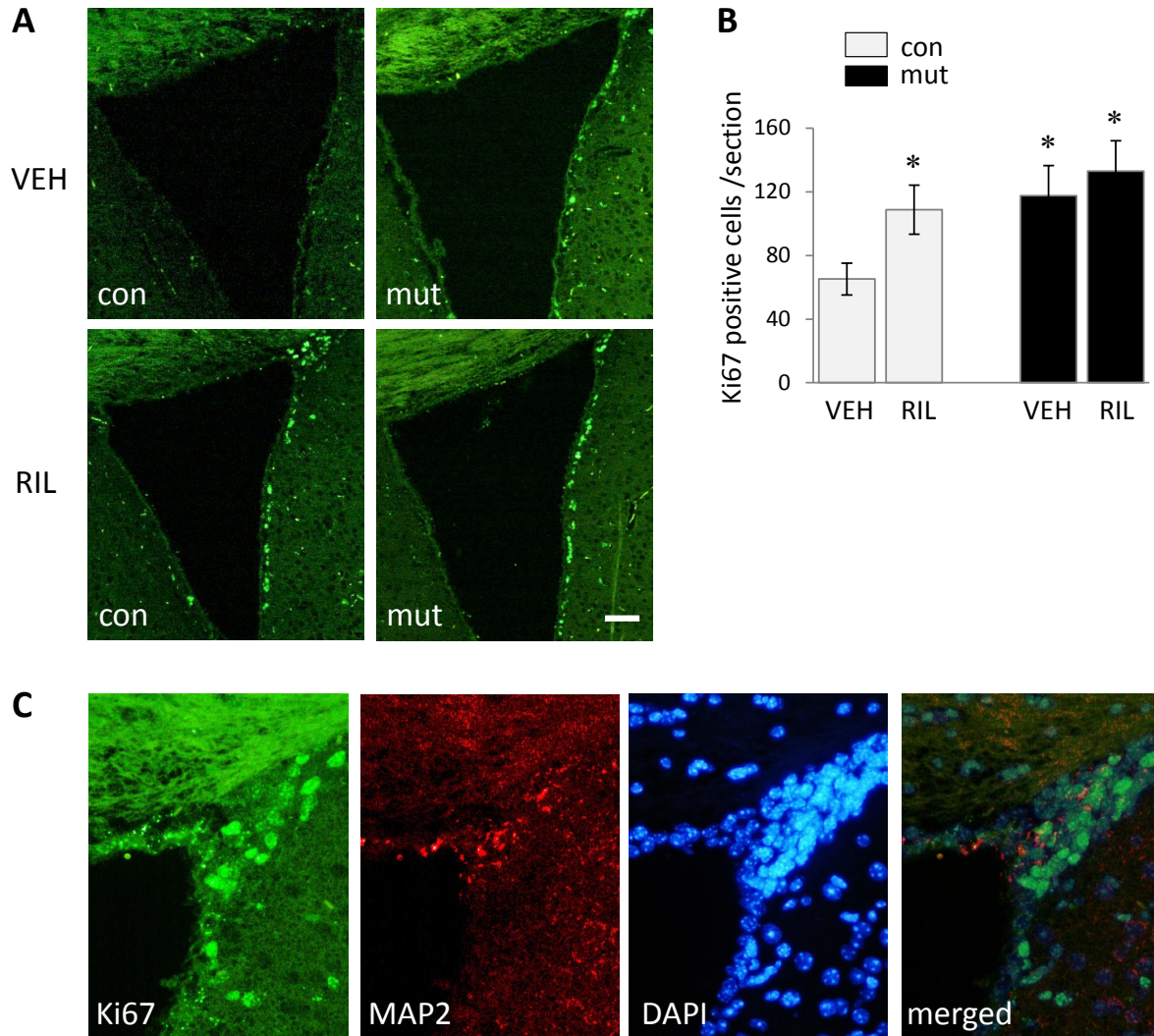
320

321 **Fig. 1.** The summary of experimental design. The mice were treated with riluzole (5 mg/kg, i.p.)
322 starting 6-th week of age. The phenotype of riluzole treated vs non-treated animals was
323 compared at 13-th week of age on behavioral and immunohistochemical level, when the effects
324 of the mutation are clearly manifested in neuronal cell loss and behavioral impairment. Ki67
325 expression and dendritic spines morphology were assessed at 9-th week when cell loss in mutant
326 animals have not yet been observed.



327

328 **Fig. 2.** Representative images of immunofluorescent analysis and quantification of proliferating
329 cells in the region of the SVZ as revealed by the Ki67 marker in control (con) and TIF-IA^{D1RCre-}
330 mutant (mut) riluzole treated and non-treated mice (**A, B**). Example of Ki67, MAP2 and DAPI
331 triple-staining carried out to confirm nuclear localization and neuronal origin of Ki67 signal (**C**).
332 Numbers of Ki67+ cells are represented by means±S.E.M. (n = 4–6; * p < 0.05 vs. con/VEH).
333 RIL – riluzole, VEH – vehicle. Scale bars: 50 µm.



334

335

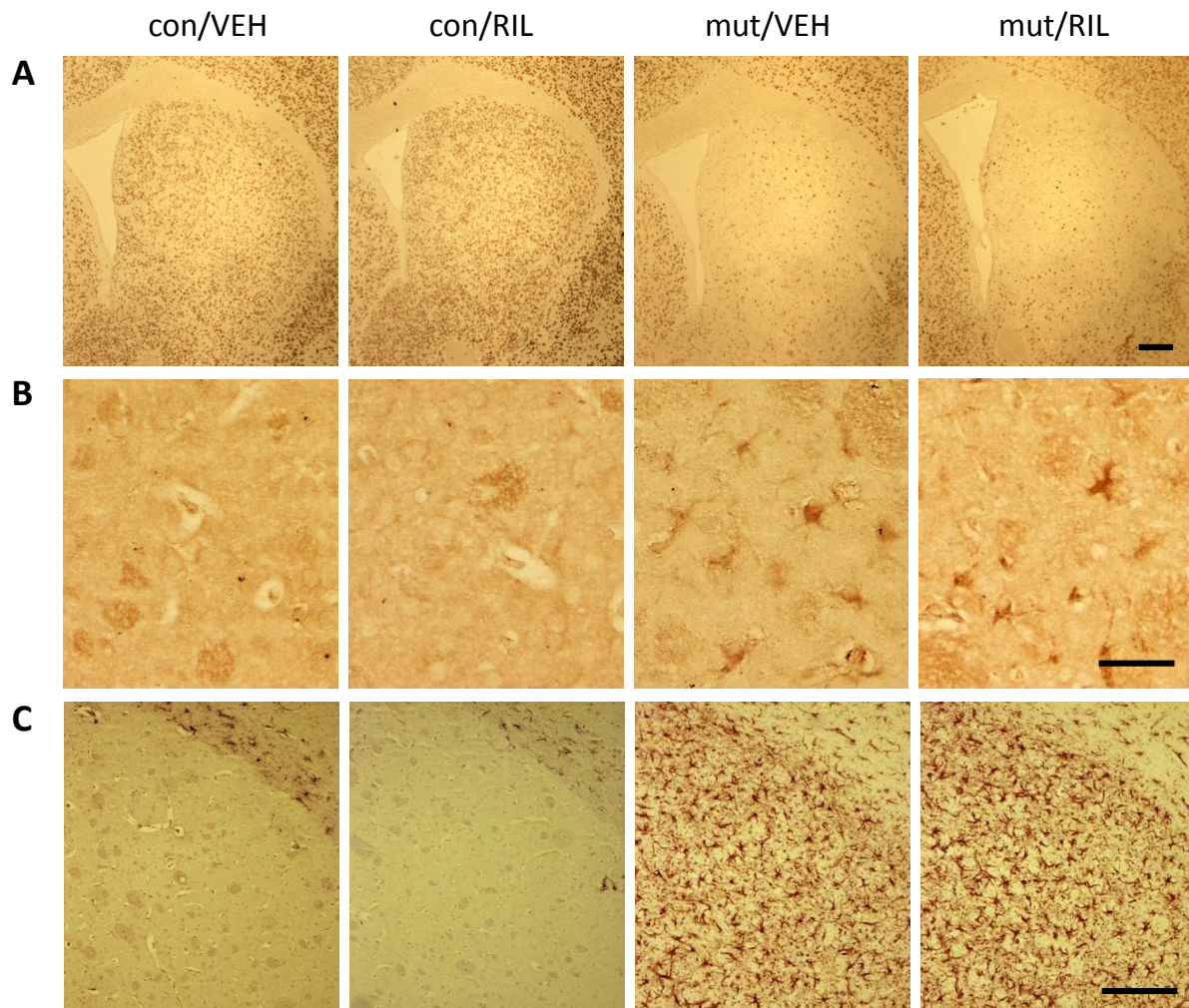
336

337

338

339

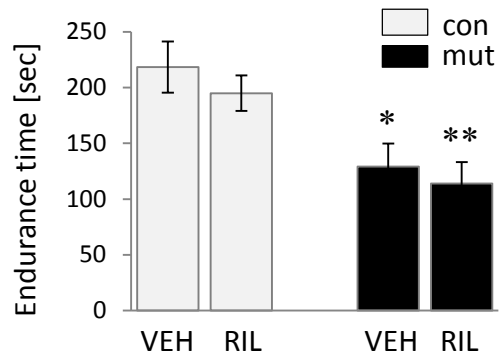
340 **Fig. 3.** Representative images of immunohistochemical analysis showing staining of striata with
341 the NeuN (**A**), induction of oxidative stress detected by the anti-8OHdG antibody (**B**),
342 astrogliosis visualized by the GFAP-specific antibody (**C**) in control (con) and TIF-1A^{DIRCre-}
343 mutant (mut) mice. RIL – riluzole, VEH – vehicle. Scale bars: 5 μ m (**A, C**), 25 μ m (**B**).



344

345

346 **Fig. 4.** Assessment of motor coordination of control (con) and TIF-IA^{D1RCre}-mutant (mut) mice
347 demonstrated by endurance in the rotarod test. Values for endurance time are represented by
348 means±S.E.M. (n = 7–8; * p < 0.05; ** p < 0.01 vs. con/VEH). RIL – riluzole, VEH – vehicle.



349

350

351 **Fig. 5.** Visualization (A-B) and quantification (C) of dendritic spines in the control (con) and
 352 TIF-1A^{DIRCre}-mutant (mut) mice. The spines were counted in the dorsal striatum (Bregma 1.1 –
 353 0.0). Data are represented by the means±SEM (n = 3–4). RIL – riluzole, VEH – vehicle.

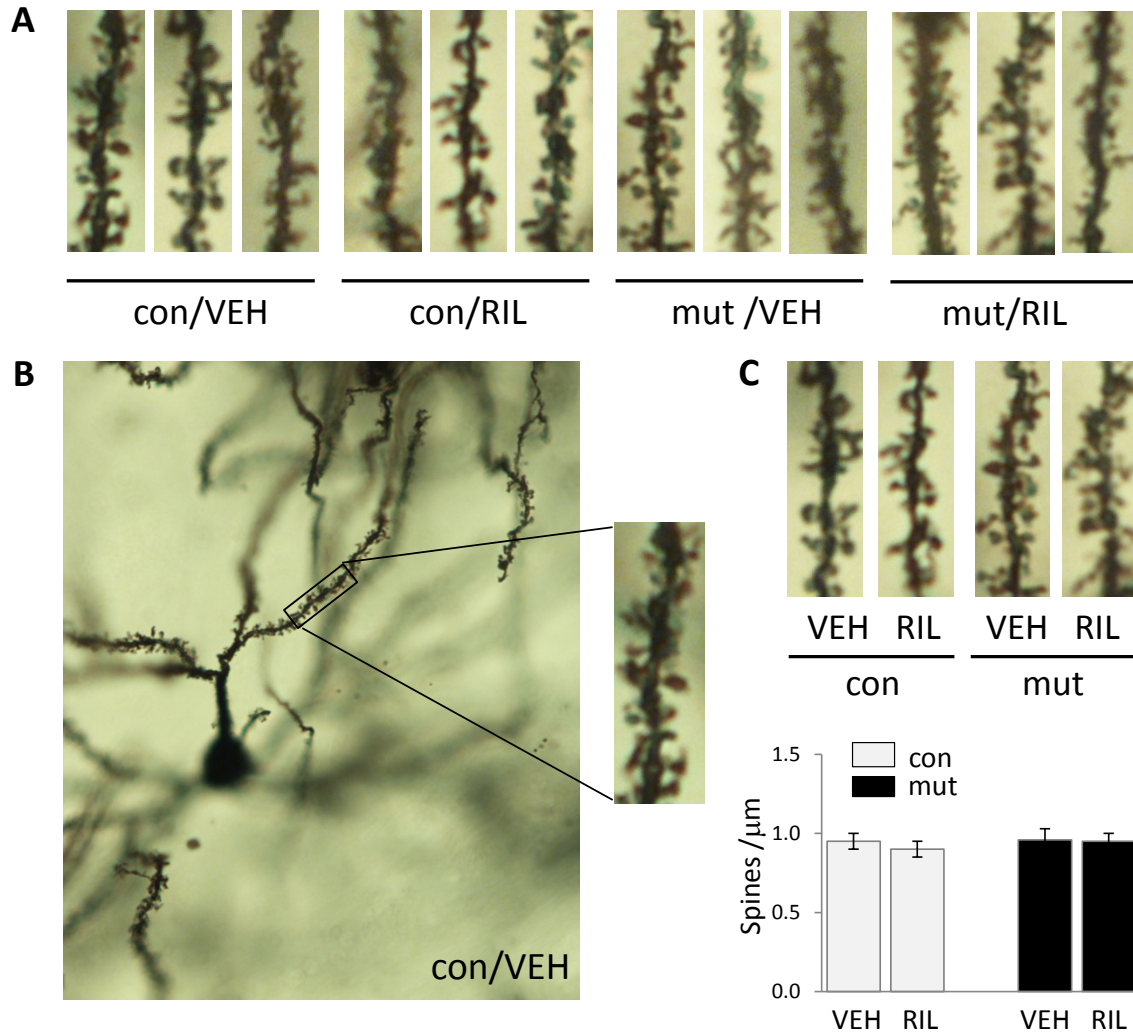


Fig. 5

354

355

356 **References**

- 357 Abdipranoto A, Wu S, Stayte S, and Vissel B. 2008. The role of neurogenesis in neurodegenerative
358 diseases and its implications for therapeutic development. *CNS Neurol Disord Drug Targets*
359 7:187-210.
- 360 Bergerot A, Shortland PJ, Anand P, Hunt SP, and Carlstedt T. 2004. Co-treatment with riluzole and
361 GDNF is necessary for functional recovery after ventral root avulsion injury. *Exp Neurol*
362 187:359-366.
- 363 Besheer J, Lepoutre V, and Hodge CW. 2009. Preclinical evaluation of riluzole: assessments of ethanol
364 self-administration and ethanol withdrawal symptoms. *Alcohol Clin Exp Res* 33:1460-1468.
- 365 Bonfanti L, and Peretto P. 2007. Radial glial origin of the adult neural stem cells in the subventricular
366 zone. *Prog Neurobiol* 83:24-36.
- 367 Carbone M, Duty S, and Rattray M. 2012. Riluzole neuroprotection in a Parkinson's disease model
368 involves suppression of reactive astrogliosis but not GLT-1 regulation. *BMC Neurosci* 13:38.
- 369 Chmielarz P, Kreiner G, Kot M, Zelek-Molik A, Kowalska M, Baginska M, Daniel WA, and Nalepa I.
370 2015. Disruption of glucocorticoid receptors in the noradrenergic system leads to BDNF up-
371 regulation and altered serotonergic transmission associated with a depressive-like phenotype in
372 female GR(DBHCre) mice. *Pharmacol Biochem Behav* 137:69-77.
- 373 Chmielarz P, Kusmierczyk J, Parlato R, Schutz G, Nalepa I, and Kreiner G. 2013. Inactivation of
374 glucocorticoid receptor in noradrenergic system influences anxiety- and depressive-like behavior
375 in mice. *PLoS One* 8:e72632. 10.1371/journal.pone.0072632
- 376 Dickstein DL, Brautigam H, Stockton SD, Jr., Schmeidler J, and Hof PR. 2010. Changes in dendritic
377 complexity and spine morphology in transgenic mice expressing human wild-type tau. *Brain*
378 *Struct Funct* 214:161-179.
- 379 Doble A. 1996. The pharmacology and mechanism of action of riluzole. *Neurology* 47:S233-241.
- 380 Emsley JG, Mitchell BD, Kempermann G, and Macklis JD. 2005. Adult neurogenesis and repair of the
381 adult CNS with neural progenitors, precursors, and stem cells. *Prog Neurobiol* 75:321-341.
- 382 Frank S. 2014. Treatment of Huntington's disease. *Neurotherapeutics* 11:153-160.
- 383 Fumagalli E, Bigini P, Barbera S, De Paola M, and Mennini T. 2006. Riluzole, unlike the AMPA
384 antagonist RPR119990, reduces motor impairment and partially prevents motoneuron death in the
385 wobbler mouse, a model of neurodegenerative disease. *Exp Neurol* 198:114-128.
- 386 Gauthier LR, Charrin BC, Borrell-Pages M, Dompierre JP, Rangone H, Cordelieres FP, De Mey J,
387 MacDonald ME, Lessmann V, Humbert S, and Saudou F. 2004. Huntingtin controls neurotrophic
388 support and survival of neurons by enhancing BDNF vesicular transport along microtubules. *Cell*
389 118:127-138.
- 390 Ginsberg G, and Lowe S. 2002. Cost effectiveness of treatments for amyotrophic lateral sclerosis: a
391 review of the literature. *Pharmacoeconomics* 20:367-387.
- 392 Hannan AJ. 2005. Novel therapeutic targets for Huntington's disease. *Expert Opin Ther Targets* 9:639-
393 650.
- 394 Hockly E, Tse J, Barker AL, Moolman DL, Beunard JL, Revington AP, Holt K, Sunshine S, Moffitt H,
395 Sathasivam K, Woodman B, Wanker EE, Lowden PA, and Bates GP. 2006. Evaluation of the
396 benzothiazole aggregation inhibitors riluzole and PGL-135 as therapeutics for Huntington's
397 disease. *Neurobiol Dis* 21:228-236.

- 398 Katoh-Semba R, Asano T, Ueda H, Morishita R, Takeuchi IK, Inaguma Y, and Kato K. 2002. Riluzole
399 enhances expression of brain-derived neurotrophic factor with consequent proliferation of granule
400 precursor cells in the rat hippocampus. *FASEB J* 16:1328-1330.
- 401 Kazantsev AG, and Hersch SM. 2007. Drug targeting of dysregulated transcription in Huntington's
402 disease. *Prog Neurobiol* 83:249-259.
- 403 Kee N, Sivalingam S, Boonstra R, and Wojtowicz JM. 2002. The utility of Ki-67 and BrdU as
404 proliferative markers of adult neurogenesis. *J Neurosci Methods* 115:97-105.
- 405 Kitzman PH. 2009. Effectiveness of riluzole in suppressing spasticity in the spinal cord injured rat.
406 *Neurosci Lett* 455:150-153.
- 407 Kreiner G. 2015. Compensatory mechanisms in genetic models of neurodegeneration: are the mice better
408 than humans? *Front Cell Neurosci* 9:56.
- 409 Kreiner G, Bierhoff H, Armentano M, Rodriguez-Parkitna J, Sowodniok K, Naranjo JR, Bonfanti L, Liss
410 B, Schutz G, Grummt I, and Parlato R. 2013. A neuroprotective phase precedes striatal
411 degeneration upon nucleolar stress. *Cell Death Differ* 20:1455-1464.
- 412 Limpert AS, Mattmann ME, and Cosford ND. 2013. Recent progress in the discovery of small molecules
413 for the treatment of amyotrophic lateral sclerosis (ALS). *Beilstein J Org Chem* 9:717-732.
- 414 Lindvall O, and Kokaia Z. 2010. Stem cells in human neurodegenerative disorders--time for clinical
415 translation? *J Clin Invest* 120:29-40.
- 416 Luzzati F, De Marchis S, Parlato R, Gribaudo S, Schutz G, Fasolo A, and Peretto P. 2011. New striatal
417 neurons in a mouse model of progressive striatal degeneration are generated in both the
418 subventricular zone and the striatal parenchyma. *PLoS One* 6:e25088.
- 419 Miller RG, Mitchell JD, and Moore DH. 2012. Riluzole for amyotrophic lateral sclerosis (ALS)/motor
420 neuron disease (MND). *Cochrane Database Syst Rev*:CD001447.
- 421 Nato G, Caramello A, Trova S, Avataneo V, Rolando C, Taylor V, Buffo A, Peretto P, and Luzzati F.
422 2015. Striatal astrocytes produce neuroblasts in an excitotoxic model of Huntington's disease.
423 *Development* 142:840-845.
- 424 Nithianantharajah J, Barkus C, Vijiaratnam N, Clement O, and Hannan AJ. 2009. Modeling brain reserve:
425 experience-dependent neuronal plasticity in healthy and Huntington's disease transgenic mice. *Am*
426 *J Geriatr Psychiatry* 17:196-209.
- 427 Parlato R, Kreiner G, Erdmann G, Rieker C, Stotz S, Savenkova E, Berger S, Grummt I, and Schutz G.
428 2008. Activation of an endogenous suicide response after perturbation of rRNA synthesis leads to
429 neurodegeneration in mice. *J Neurosci* 28:12759-12764.
- 430 Rafa-Zablocka K, Jurga A, Bagińska M, Parlato R, Schütz G, Nalepa I, and Kreiner G. 2014. Involvement
431 of noradrenergic system in Parkinson's disease – study on novel transgenic mouse models. *Eur*
432 *Neuropsychopharmacol* 24:S642-S643
- 433 Ransome MI, Renoir T, and Hannan AJ. 2012. Hippocampal neurogenesis, cognitive deficits and
434 affective disorder in Huntington's disease. *Neural Plast* 2012:874387.
- 435 Rieker C, Engblom D, Kreiner G, Domanskyi A, Schober A, Stotz S, Neumann M, Yuan X, Grummt I,
436 Schutz G, and Parlato R. 2011. Nucleolar disruption in dopaminergic neurons leads to oxidative
437 damage and parkinsonism through repression of mammalian target of rapamycin signaling. *J*
438 *Neurosci* 31:453-460.
- 439 Sarnat HB. 2013. Clinical neuropathology practice guide 5-2013: markers of neuronal maturation. *Clin*
440 *Neuropathol* 32:340-369.

- 441 Schmidt J, Schmidt T, Golla M, Lehmann L, Weber JJ, Hubener-Schmid J, and Riess O. 2016. In vivo
442 assessment of riluzole as a potential therapeutic drug for spinocerebellar ataxia type 3. *J*
443 *Neurochem* 138:150-162.
- 444 Sepulveda J, Astorga JG, and Contreras E. 1999. Riluzole decreases the abstinence syndrome and
445 physical dependence in morphine-dependent mice. *Eur J Pharmacol* 379:59-62.
- 446 Simard JM, Tsybalyuk O, Keledjian K, Ivanov A, Ivanova S, and Gerzanich V. 2012. Comparative
447 effects of glibenclamide and riluzole in a rat model of severe cervical spinal cord injury. *Exp*
448 *Neurol* 233:566-574.
- 449 Spires TL, Grote HE, Garry S, Cordery PM, Van Dellen A, Blakemore C, and Hannan AJ. 2004.
450 Dendritic spine pathology and deficits in experience-dependent dendritic plasticity in R6/1
451 Huntington's disease transgenic mice. *Eur J Neurosci* 19:2799-2807.
- 452 Squitieri F, Ciammola A, Colonnese C, and Ciarmiello A. 2008. Neuroprotective effects of riluzole in
453 Huntington's disease. *Eur J Nucl Med Mol Imaging* 35:221-222.
- 454 Tunez I, Tasset I, Perez-De La Cruz V, and Santamaria A. 2010. 3-Nitropropionic acid as a tool to study
455 the mechanisms involved in Huntington's disease: past, present and future. *Molecules* 15:878-
456 916.
- 457 Verhave PS, Jongsma MJ, Van Den Berg RM, Vanwersch RA, Smit AB, and Philippens IH. 2012.
458 Neuroprotective effects of riluzole in early phase Parkinson's disease on clinically relevant
459 parameters in the marmoset MPTP model. *Neuropharmacology* 62:1700-1707.
- 460 Veyrac A, Sacquet J, Nguyen V, Marien M, Jourdan F, and Didier A. 2009. Novelty determines the
461 effects of olfactory enrichment on memory and neurogenesis through noradrenergic mechanisms.
462 *Neuropsychopharmacology* 34:786-795.
- 463 Yuan X, Zhou Y, Casanova E, Chai M, Kiss E, Grone HJ, Schutz G, and Grummt I. 2005. Genetic
464 inactivation of the transcription factor TIF-IA leads to nucleolar disruption, cell cycle arrest, and
465 p53-mediated apoptosis. *Mol Cell* 19:77-87.

466

467